Photochromicity and Fluorescence Lifetimes of Green Fluorescent Protein

George Striker,* Vinod Subramaniam,* Claus A. M. Seidel, and Andreas Volkmer†

Max Planck Institute for Biophysical Chemistry, Am Fassberg 11, D-37077 Göttingen, Germany

Received: April 29, 1999; In Final Form: August 3, 1999

The green fluorescent protein (GFP) of the bioluminescent jellyfish *Aequorea* and its mutants have gained widespread usage as an indicator of structure and function within cells. Proton transfer has been implicated in the complex photophysics of the wild-type molecule, exhibiting a protonated A species excited at 400 nm, and two deprotonated excited-state species I* and B* with red-shifted excitation ∼475 nm. Photochromicity between the protonated and deprotonated species has been reported upon 400 nm excitation. Using precise time-resolved spectroscopy, we have been able to distinguish the fluorescence lifetimes of the I and B species (∼3.3 and ∼2.8 ns, respectively) and show that the irreversible photochromicity which we observe is due to formation in the excited state of the B species, which cannot return to other species in the ground state. The ground state A and I species are in thermal equilibrium. Anisotropy measurements indicate that the chromophore lies rigidly in the molecule with a rotational correlation time of ∼15.5 ns, as is to be expected for a molecule of this size. Time-resolved measurements of enhanced yellow fluorescent protein (EYFP) and red-shifted green fluorescent protein (RSGFP) were also analyzed.

Introduction

The *Aequorea* green fluorescent protein (GFP) has rapidly developed from a rarity of nature—a protein involved in the visible bioluminescence of the jellyfish *Aequorea*—to a tremendously popular research tool in cellular, molecular, and developmental biology. The ability to fuse GFP to proteins of interest and express the constructs in vivo allows GFP to be used as a versatile indicator of structure and function within cells by visualization with standard microscopy techniques. The pace of development and application of mutants of GFP expressing different spectral and photophysical characteristics has far outstripped the corresponding efforts on their chemical and physical characterization. The popularity of GFP and its mutants as fluorophores requires careful study of their photophysical properties.

Since the pioneering work of Ward[1] and Prendergast[2] in the 1980s, there have been relatively few studies of the rich photophysical properties of this protein. Chattoraj et al.[3] showed that the green fluorescence was the result of a deprotonation process in the excited state, leading from the most populated A state of the protein, with its excitation peak at 397 nm, to a deprotonated and thus charged excited "intermediate" state I*, as well as to a likewise deprotonated but more stable B* state. The corresponding ground states (I,B) were thought to account for the secondary excitation peak at 476 nm. Lossau et al.[4] primarily studied the complex and very fast kinetics (femtosecond to several picoseconds) of the deprotonation reactions by ultrafast time-resolved fluorescence and absorption studies. Recently, Creemers et al.,[5] from hole-burning spectroscopy at cryo-temperatures (1.6 ° K), were able to explicitly distinguish the three ground states and determine their 0−0 transitions (434 nm for A, 477 nm for B, 495 nm for I).

Conventional time-resolved spectroscopy in these papers had established a lifetime of ∼3 ns for all decays in the green part of the spectrum, with no differentiation between the species,[4,6] in addition to picosecond times associated with the deprotonation. Thus, little was known about the relative populations in the ground state at room temperature. We conjectured that very precise time-resolved fluorescence experiments might separate these species and give more detailed information on the inherent processes. During these investigations it also became apparent that a property that originally led to difficulties in the study—the extreme photochromicity of wtGFP when excited at 400 nm, already reported[3,7,8]—could actually be used to gain a better understanding of the data.

Our data suggest that wtGFP clearly exhibits multiexponential fluorescence decays at all excitation wavelengths and that the photochromicity effect does not alter the fluorescence lifetimes, but rather just the pre-exponential factors (amplitudes). This allows us to assign the lifetimes found to the various species. Similar multiexponential decays were found for the two mutant proteins studied, EYFP and RSGFP, but here no photochromic effect could be provoked, although these had been reported.[9,10]

Materials and Methods

DNA encoding for wild-type GFP (wtGFP) and the mutants RSGFP[11] and EYFP (Clontech, USA) was cloned into the plasmid pRSETa (Invitrogen, USA). The mutants carry the following changes in the protein sequence: RSGFP (Phe64 → Met, Ser65 → Gly, Glu69 → Leu) and EYFP (Ser65 → Gly, Val68 → Leu, Ser72 → Ala, Thr203 → Tyr). The recombinant plasmids allow expression of modified GFPs containing six histidines at the amino terminus under control of the T7 promoter, which is inducible by isopropyl-D-thiogalactoside (IPTG). GFP positive bacteria were selected with Ampicillin. The recombinant plasmids were transformed into *E. coli* BL21 (DE3) cells. Cells were cultured in LB medium supplemented with Ampicillin and grown to an $A_{600} \approx 0.6$, at which point protein expression was induced using IPTG. Cells were typically grown further for 4 h following induction. The recombinant proteins with a six-histidine tag were purified on a Ni-chelating

* Corresponding authors. Email: gstrike@gwdg.de; vsubram@gwdg.de.
† Current address: Department of Chemistry and Chemical Biology, Harvard University, 12 Oxford Street, Cambridge, MA 02138.

10.1021/jp991425e CCC: $18.00
Published on Web 09/21/1999

resin (Ni−NTA−Agarose, Qiagen, Hilden, Germany) using standard procedures. Further purification by gel filtration was performed when required. All proteins were dissolved in 10 mM Tris−HCl buffer, pH 8, containing 100 mM NaCl. Protein concentrations ranged between 250 nM and 1 μM.

Excitation at 476, 496, 502, and 528 nm was achieved with an Ar^+ laser (Sabre, Coherent, Palo Alto, CA) actively mode-locked (Pulse Drive, APE, Berlin, Germany) at 73 MHz. Reduction to 4.56 MHz with an acousto-optical modulator (pulse-picker by Coherent, Palo Alto, CA) yielded pulses of approximately 180 ps (fwhm). Two-photon excitation at 800 nm was with a Ti:sapphire mode-locked laser system (Mira 900, Coherent, Palo Alto CA) at 800 nm with a repetition rate of 76 MHz (pulse fwhm: 200 fs). For excitation at 400 nm, the Ti: sapphire fundamental was frequency doubled.

Laser pulses were passed through a quartz quarter-wave plate (Steeg & Reuter, Giessen, Germany) and a Glan polarizer (Halle Nachf., Berlin, Germany) to produce a vertically polarized excitation beam. The emission polarizer was oriented at the magic angle (54.7°), parallel or perpendicular to the excitation. Emission wavelengths were selected by a subtractive double monochromator (home-built), which was imaged onto a peltier-cooled microchannel plate photomultiplier (MCP-PM U 3809, Hamamatsu, Japan).

The MCP-PM signal was amplified with a fast rise time amplifier (home-built), shaped in a constant fraction discriminator (TC 454 Quad, Tennelec, Oak Ridge, TN), and directed to a time-to-amplitude converter (TAC TC 862, Tennelec, Oak Ridge, TN) as start pulses. Stop pulses were generated by a Si-photodiode (PHD 400, Becker & Hickel, Berlin, Germany) monitoring the excitation laser beam. The output pulses were shaped as before and delayed. The analogue TAC signals were digitized using a 16 bit analog-to-digital converter (ADC 7423 UHS-s, Silena, Milano, Italy) and stored in a PC. The fwhm of the experimental instrument response function obtained was typically 200 ps for both Ar^+ and Ti:sapphire laser excitation. The data were collected in 4 K channels at 3.4 ps/ch. All measurements were taken at ambient temperature in a lab climatized at 17 °C and lasted from several hours to overnight, in cycles of typically 180 s per wavelength or polarization orientation. Intermediate records were stored on disk.

Bleaching was either accomplished by laser excitation during lifetime measurements or with a xenon lamp (HBO 100W/2 Osram, Munich, Germany) and band-pass interference filters (Schott, Mainz, Germany) with half-widths $\approx$ 20 nm, maxima as given in Experimental Section, and spectra measured with a SLM 8000C spectrometer (SLM Instruments, Urbana-Champaign, IL), with corrections for excitation and emission channels.

The software system for analysis of time- and anisotropy-resolved fluorescence experiments[12,13] (called sandbox) was rewritten in C and can typically globally analyze 10 records with 4000 channels each. Initial analysis uses the improved modulating functions method[12] (requiring no initial guess), which is then refined using nonlinear least-squares analysis. Quality of fit is judged by the χ^2 value, weighted deviations, and their autocorrelations. The sandbox contains a routine to correct for nonlinearity in the TAC by using the integral of a linearity curve, collected overnight from random incident light stopping the TAC at the laser frequency, as a time axis. This was particularly necessary for 76 MHz records, but also improved other fits. When the repetition rate is high with respect to the lifetimes, so that fluorescence is still present upon arrival of the next flash, the convolution routine carries the remaining signal to the beginning of the cycle. The sandbox includes a facility to correct for possible scatter light which also effectively corrects for signals (fluorescence or uprise) too fast for the instrumentation. For two-photon excitation, the scatter signal is squared. For anisotropy analysis, a synthetic anisotropy numerator record ($\| - \perp$) along with a weighting record is created by fitting a linear combination of $\|$ and $\perp$ to the magic angle record. Analysis of this record yields rotational correlation times ρ as inverse differences and initial anisotropies as quotients, when compared to the analysis of the magic-angle record.

As noted above, the appearance of the autocorrelation, which should remain close to the axis and repeatedly cross it (cf. Figure 2), was regularly used to judge the quality of a fit. Low χ^2 values do not necessarily indicate this. This appearance can be quantified by a somewhat equivalent numerical procedure,[14] counting the number of runs (essentially crossing of the baseline) of the deviates. The expected number of runs is

$$\mu = \frac{2n_1n_2}{n_1 + n_2} + 1$$

where n_1 and n_2 are the number of deviates above and below zero, respectively, and the variance is given by

$$\sigma^2 = \frac{2n_1n_2(2n_1n_2 - n_1 - n_2)}{(n_1 + n_2)^2(n_1 + n_2 - 1)}$$

Thus, the deviation of the fit can be found as a multiple of σ. This method is intended for statistically independent trials, such as the tossing of a coin. Because we are working partially with analogue electronics, in particular the TAC, which always has a certain amount of nonlinearity (as seen in the fact that the autocorrelation curves do not go to zero sharply but just gradually; see Figures 2 and 3), we cannot apply this test to successive channels, but must always compare channels a certain distance apart. We have chosen 75 channels ($\sim$250 ps).

Lifetime-resolved spectra are displayed by plotting the absolute amplitudes of a global experiment against the emission wavelengths. Bleaching effects, i.e., changes in the amplitudes of the various components, are displayed by globally analyzing a set of intermediate records and plotting absolute amplitudes as a function of number of cycles.

The accuracy of the data acquisition and analysis were verified measuring several small dye molecules whose lifetimes were known from the literature. The expected lifetimes and anisotropies were obtained.

Results

Bleaching and Photochromicity. Figure 1 shows excitation and emission spectra of wild-type green fluorescent protein (wtGFP), enhanced yellow fluorescent protein (EYFP), and red-shifted green fluorescent protein (RSGFP). While EYFP and RSGFP have excitation maxima at 515 and 490 nm, respectively, and excitation shoulders at 476 and 465 nm, wtGFP has two excitation maxima at 398 and 476 nm. To test the photochromicity, we illuminated all three proteins at the maxima and shoulders.

After 4 h of illumination at 476 nm, the wtGFP sample of Figure 1a had excitation (λ_{em}= 500, 514, and 530 nm) and emission spectra (λ_{ex} = 400 and 476 nm) reduced by $\sim$30%. But in every case these spectra were essentially congruent to the original spectra when scaled by the integral. The sample recovered from this bleaching with a half-life of $\sim$40 h.

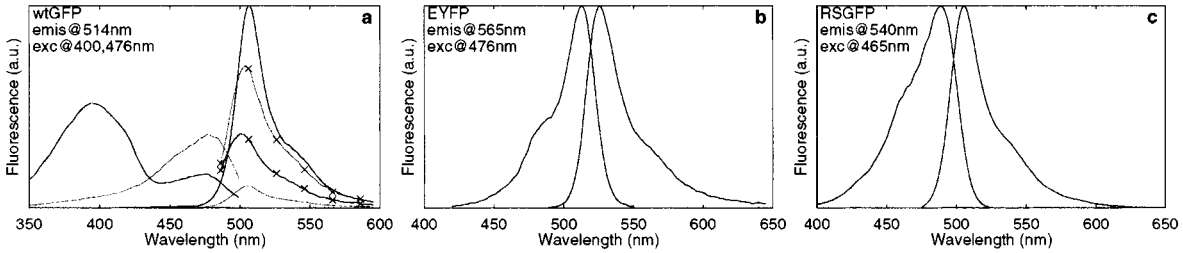

Figure 1. Fluorescence excitation and emission spectra of (a) wtGFP, (b) EYFP, and (c) RSGFP at the emission and excitation wavelengths indicated. Additionally, in (a), where excitation of the native protein has been plotted black, the corresponding emission after 4 h illumination at 400 nm is shown as dotted lines. The native emission excited at 476 nm is marked with ×, as is the (enhanced) emission at 476 nm after illumination. All spectra have been smoothed.

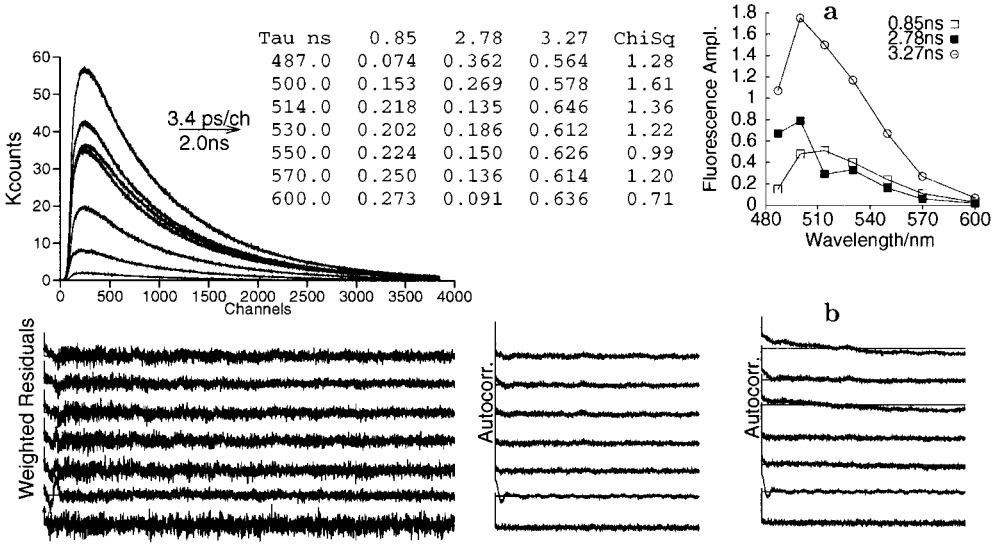

Figure 2. Time-resolved fluorescence of wtGFP excited at 476 nm and measured at 487, 500, 514, 530, 550, 570, and 600 nm, globally analyzed. The partial amplitudes at each wavelength are tabulated. Simulated data is plotted through the measured data, weighted residuals, and their autocorrelations below. The disturbance near zero at 570 nm is due to Raman scattering. The maximal data plot is at 500 nm, followed by increasing wavelengths, except that 487 nm is just above 530 nm. Inset 2a: lifetime-resolved spectra of the analysis of Figure 2, showing the absolute amplitudes of the three components at the various wavelengths. Note that the fluorescence emission from a component is the product of the amplitude and lifetime. The number of runs (see Methods) is less than one standard deviation below expectancy for the three exponential fit (12 951 runs against 12 977 expected in the seven traces). Inset 2b: the autocorrelations of the same experiment as Figure 2, but with the best two-component fit (860 ps, 3.16 ns). The number of runs is off by 77 standard deviations (only 6565 runs). No fit is possible without a time close to 850 ps.

A sample of wtGFP was subjected to 4 h illumination at 400 nm. Now a photochromic effect was observed (Figure 1a). The excitation spectra (λ_{em} = 514 nm) showed that the emission intensity at 400 nm was reduced more than 85%, while at 476 nm the emission doubled and was red-shifted. We attempted to revert this effect, first by keeping the protein in the dark at cool temperatures (4 °C), then at room temperature. We also tried exposing it to 476 nm light, and finally tried further warming. Taking the ratio of the fluorescence excitation peak at 476 nm to that at 400 nm as a measure, the sample recovered just 1% after 40 h at 4 °C, another 0.5% after 30 min intense illumination at 476 nm (leading to bleaching of the entire curves but, by our criterion, without effect on photochromicity). Another 1% recovery occurred after leaving the sample overnight at 20 °C and then 24 h at 40 °C, and 5 h at 70 °C reduced the total fluorescence (measured at 20 °C) of the sample well over 60%, but the photochromicity was still more than 90%. Thus, we found essentially no recovery of wtGFP after photoconversion over a number of days.

We also illuminated EYFP and RSGFP for several hours near their respective excitation maxima (515 and 490 nm) and at the shoulders (476 and 465 nm). In each case we observed bleaching, but retrieved excitation and emission spectra at maxima and shoulders that were essentially congruent (after normalization) immediately following illumination and again after partial recovery. These proteins thus showed no evidence of photochromicity under these conditions.

Time-Resolved Measurements at 476 nm. Global analysis of the time-resolved fluorescence of wtGFP excited at the minor peak of excitation at 476 nm clearly indicated two different lifetimes close to 3 ns, one shorter, ∼2.8 ns, and one longer, ∼3.3 ns (Figure 2). The amplitude (pre-exponential factor) of the latter is more than twice that of the shorter time through most of the spectrum. Both show a maximum at 500 nm, but whereas the 3.3 ns component continuously decreases toward the red, the 2.8 ns component shows a local minimum at 514 nm, and then increases toward 530 nm before diminishing. We note that this minimum at 514 nm, although not deep, was repeatedly found in a number of similar experiments with different samples. In addition we find a shorter component of 850 ps lifetime, where the amplitude of this lifetime is small, but not stable between experiments with different samples of wtGFP. In some experiments this component was only found when coanalyzed with other experiments, and then with a very small amplitude. Additionally, as stated in Materials and Methods, there are indications of very fast components outside of the resolution of these experiments.

Time-resolved fluorescence was also carried out on a sample of wtGFP exciting at 476 nm after prolonged exposure to 400 nm radiation, thus (see Figure 1a, dotted lines) at a wavelength

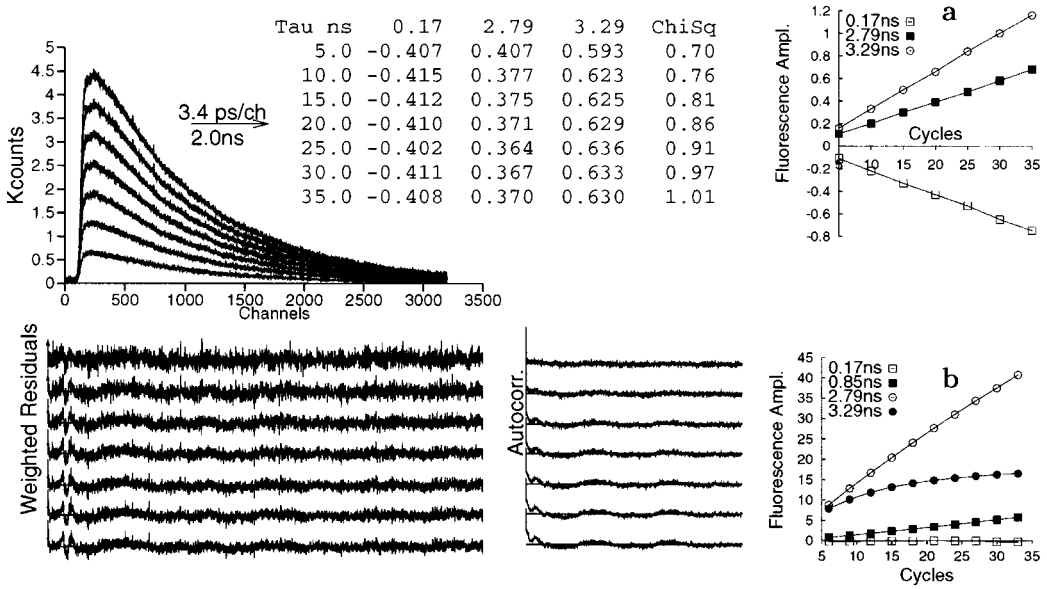

Figure 3. Time-resolved fluorescence of wtGFP with two-photon excitation at 800 nm and measured at 514 nm. The plot shows the cumulative data set every five cycles of measurement, globally analyzed. Otherwise same as Figure 2. Inset 3a: plot of the cumulative amplitudes from the analysis of Figure 3. There is no indication of bleaching or photochromicity in this two-photon experiment at low count rate. Inset 3b: plot of the cumulative amplitudes from analysis (not shown) of a single photon time-resolved fluorescence experiment with wtGFP excited at 400 nm, measured at 514 nm, over 33 cycles, showing the photochromicity. The maximum channel in the final record had 128 000 counts. There is considerable photochromicity before the first cycle due to the setup time of the experiment, during which the sample was illuminated.

with greatly increased total fluorescence. We found that the 3.3 ns component decreases drastically, but that it is the 2.8 ns component that increases correspondingly and accounts for the increase in fluorescence. The 850 ps component also increases. The minimum of the 2.8 ns component at 514 nm disappears.

Time-Resolved Measurements at 400 and 800 nm. Time-resolved fluorescence at 400 nm excitation was carried out at the full mode-locked frequency of 76 MHz. As expected, the "bleaching" of the fluorescence excited at this wavelength created a problem. Nevertheless, all three components found at 476 nm excitation appeared, although the 850 ps component was not present until some bleaching had taken place. The 3.3 ns component decreased rapidly so that emission wavelength dependence of the amplitudes could not be evaluated. In another experiment monitoring just the 514 nm emission, the rapid decay of the 3.3 ns component was seen accompanied by a far smaller but equally fast increase of the 850 ps component, while the 2.8 ns component remained essentially unchanged (see Figure 3b).

Two-photon excitation of GFP's has been established.[15,16] In the measurement shown in Figure 3, we used two-photon excitation with low count rates at 800 nm (with constant magnetic stirring of the solution) and recorded just the 514 nm emission. There was no sign of bleaching during the experiment (Figure 3a), and the amplitude of the 3.3 ns component was 1.7 times that of the 2.8 ns component. The 850 ps component was not present. A strong component with negative amplitude (growing-in) at 170 ps was required for the fit. Although this two-photon record had only 4.5 K-counts at the peak, its 4.7 M-counts integrated over 4000 channels rendered it reliable. The 170 ps time was also present in the multiemission record, in which the amplitude was negative at 514 nm but positive elsewhere (data not shown).

Red-Edge Time-Resolved Measurements. At 528 nm excitation of wtGFP, some 60% of the amplitude appeared in a longer component of 4.5 ns. A strong component faster than our resolution was also evident. The same long time already appears upon excitation at 496.5 nm, with from 6% of the amplitude at 514 nm emission to 25% at 570 nm. It then becomes impossible to separate between two components close to 3 ns.

Anisotropy. The anisotropy of wtGFP was measured at most excitation and emission wavelengths (except 400 nm OPE and 800 nm TPE excitation due to photochromicity). A rotational correlation time ρ of 15.5 ± 1 ns was consistently found, which is as great an accuracy as can be expected given a fluorescence lifetime of $\sim$3 ns and is in agreement with previous results.[6] There was no indication of multiple correlation times or a difference in correlation times between the fluorescence components. The initial anisotropy values r_0 were $\sim$0.38. Addition of 60% glycerol shortened the fluorescence lifetimes (1.7 ns (5%) and 2.8 ns (95%) in a single experiment, not fit globally with others) and led to a rotational correlation time of $>$100 ns but again without evidence of multiple rotational correlation times.

EYFP. The fluorescence lifetimes found for a yellow-emitting mutant of GFP, EYFP, are extremely similar to those of the wild-type, possibly the two lifetimes above and below 3 ns are slightly more separated (2.7 and 3.4 ns, but see Discussion). This mutant lacks the two separate excitation peaks found in the wild type, but measured at the excitation shoulder (476 nm), these two lifetimes show almost equal amplitudes. Excited at 502 nm, the amplitude ratio of the longer to shorter time increased from about 2-fold at 510 nm emission to almost 4-fold above 540 nm. Anisotropy measurements also gave results identical to the wild type.

Red Shifted GFP. Four lifetimes, 170 ps, 670 ps, 1.2 ns, and 3 ns were necessary to fit the fluorescence of RSGFP excited at 496.5 nm, with emission measured at 514, 530, 550, and 570 nm. Measurements excited at 476 nm with emission at 514 nm could be cofit with the same lifetimes. The 3 ns time was very weak (0.5% of the total amplitude at 496.5 nm, 2% at 476 nm). The bulk of the amplitude was distributed equally at 670 ps and 1.2 ns, except that the shorter time has 27% greater amplitude in a test experiment carried out at pH 5. The 170 ps

time was also weak, with a negative amplitude at 514 nm emission.

Rotational correlation times similar to those of wild-type GFP were found, but were ~2 ns shorter, i.e., ~13.5 ns. There was indication of lower r_0 values (~ 0.35), which would mean that some of the anisotropy was lost at very short times or that there was a change between absorption and emission angles. We did not find any indication of multiple rotational correlation times. Complex anisotropy decay has been reported for RSGFP excited at 400 nm.[16]

Discussion

Accuracy Considerations. Some justification is required for analyzing a number of experiments with up to four exponential components and detection of two lifetimes as close as 2.8 and 3.3 ns. Lossau et al.[4] reported 3.3 ns as the only long component of wtGFP fluorescence. They also observed lifetimes of 129 and 227 ps in two experiments with 400 nm excitation, which might correspond to our 170 ps time at that wavelength. As pointed out in the Methods section, many of the experiments analyzed in the present study contained several hundred million counts over 4000 channels. The effect of combining the two long lifetime components is seen in the autocorrelations of the best two-component fit in Figure 2b. This appearance of the autocorrelation can be quantified by counting the runs (see Materials and Methods) in the residuals; the three-exponential fit has close to the expected number of runs, while the two exponential fit has half that number. The two times, 2.8 and 3.3 ns, are the result of global analysis of individual experiments and coanalyses over a large number of experiments, which were often performed several times. We do not exclude an error of some 100 ps in these times, as the deviations do not increase drastically if the times are concurrently changed slightly with adjustment of the amplitudes. Essential for the fit is the existence of two separate times with ~500 ps separation, one above and one below 3 ns. The amplitudes (preexponential factors) are also subject to error when the lifetimes are adjusted, but their trend as a function of wavelength remains the same.

Excited-State Deprotonation. Previous studies[3,4] showed that the fluorescence properties of wtGFP are characterized by excited-state deprotonation of the chromophore. Using femtosecond time resolution, Lossau et al.[4] showed that the depopulation of the excited state of the protonated A species, A*, is far faster than could be resolved in the present study. Excited-state deprotonation leads to a charged excited state I* and partially, by "equilibration" to the excited state, B*. Each of these excited-state species have their associated ground-state species, A, I, and B, A being excited at ~400 nm and B and I at ~476 nm. (In the terminology of Lossau et al.,[4] the excited A state is RH*, the excited I state R^{-*}_{neq} and the excited B state R^{-*}_{eq}.)

The major component of 3.3 ns would reflect the decay of the I* state, a population created in the excited state in a complex process,[4] visible in our lifetime of 170 ps with negative amplitude and indications of very short times. The 2.8 ns component would either stem from some direct excitation of the B state still absorbing as low as 400 nm or some direct conversion of A* → B*, or both.

(1) This interpretation woud imply that, at equilibrium, there is a large population of the I ground state which is excited at 476 nm. The excited I* state then decays with a lifetime of 3.3 ns, while the excited state of the stable B ground state decays in 2.8 ns.

(2) Illumination at 400 nm clearly depopulates the A ground state, as seen in the excitation spectra. This had been previously reported.[3,7,8]

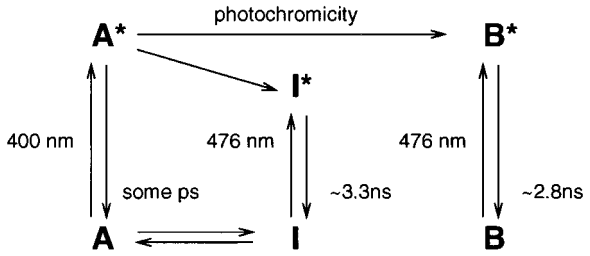

Figure 4. Scheme of the excited and ground state species of wtGFP, as found in this work. Molecules in the B or B* states cannot reach the other states (in terms of days). Ground-state A and I equilibrate, at least in minutes, and A* photoconverts by deprotonation to I* and B*. The conversion A* → B* results in photochromicity. Excitation wavelengths given are the laser lines used in our experiments, and lie close to the maxima.

(3) But, as the 3.3 ns component at 476 nm excitation is also depleted, we must surmise that there is a fast (at least in minutes) equilibration between the I and the A ground states. This equilibrium is also seen in that the bleaching at 476 nm leaves the excitation spectra unchanged in form, i.e., the excitation peak at 400 nm, which is attributable to the A state is also reduced, without direct excitation of *A*.

(4) On the other hand, we see from the stability after 400 nm bleaching that there is virtually no ground state path from B to A or I.

(5) Similarly, there is no excited-state pathway, as illumination at 476 nm does not bring back the 3.3 ns component nor the excitation at 400 nm. We can also rule out an excited-state pathway from I* → B*, as this would lead to reduction of the 3.3 ns time during illumination at 476 nm.

(6) Thus, the B* component found at 400 nm excitation must come directly from A* without an I* intermediate, and is (presumably) responsible for the photoconversion.

These processes are summarized in the scheme of Figure 4.

We note that we have adopted the established A, I, B terminology.[3] The I was to suggest a proton-deprived intermediate state, which through change of the conformation can (infrequently) progress to the stable B state.[17] Of the ionized states, the B state was detected in the crystal structure analysis of Brejc et al.[17] Our time-resolved fluorescence data suggest that the I state is independent and is not (with any reasonable probability and thus experimental effect) converted to the B state, either in the excited or in the ground state. This does not exclude the possibility of an excited-state precursor of both I and B, without an associated ground state.

There are still problems left in this interpretation. We cannot ascribe the 850 ps time, which increases under 400 nm illumination, to any known species. Furthermore, if the 2.8 ns time at 400 nm excitation were solely due to excited-state A* → B* conversion, we would expect its amplitude to decrease along with the 3.3 ns amplitude. On the other hand, if it were due to some absorption of ground-state B at this wavelength, we would expect an increase commensurate with the increase of the B ground state population. We see neither (Figure 3b), which at best we could ascribe to a fortuitious canceling out of the two processes.

These considerations indicate the possibility that this simple model does not fully describe the underlying processes. Another indication is the minimum of the amplitude of the 2.8 ns component at 514 nm upon excitation at 476 nm, with higher amplitudes on either side. This might be an indication of two distinct ground-state populations with that lifetime.

In low-temperature experiments (1.6 K, 50% glycerol), Creemers et al.[5] observe both thermal equilibration from the B

state to the A state as well as radiationless conversions from B* → I and I* → B. Our data do not support B* → I as in our experiments 476 nm radiation did not reduce B (after bleaching of *A*), and as a consequence exclude I* → B, as then 476 nm radiation would enhance B and, as a result of the thermal equilibration between I and A, reduce A. This situation need not hold, though, at grossly different temperatures and solution conditions.

A possible practical application of the virtually irreversible photochromicity described above might be found in energy-transfer experiments using wtGFP as an acceptor, in which the existence of two excitation wavelengths is detrimental. Bleaching at 400 nm would eliminate this excitation, and greatly enhance the energy transfer to the band around 476 nm.

Red-Edge Effect. Effects of exciting a chromophore at the red edge of its spectrum have been reported in connection with anisotropy[18] and relaxation phenomena,[19] primarily in more viscous solvents, and have been associated with solvent−solute relaxation and photoselection of relaxed molecules at the red edge. In the case of GFP's, where the chromophore appears to be well-protected from the solvent within the protein, we would expect such relaxation phenomena, if they exist, to lie within the molecule and be associated with reorganization of the bonds close to the chromophore.[17,20] The longer lifetime of 4.5 ns would indicate that the photoselected, more relaxed, molecules are less prone to nonradiative conversion to the ground state.

Anisotropy. According to the Einstein−Perrin equation, $\rho = V\eta/kT$, (where V = volume, η = viscosity, T = absolute temperature, and k is the Boltzmann constant), the ∼15.5 ns rotational correlation time ρ of wtGFP would correspond to a sphere of diameter ∼5 nm. The crystal structure[21,22] indicates the molecule is of cylindrical form with length 4.5 nm and diameter 2.5 nm. We cannot expect to differentiate between these objects, as seen in a fluorescence lifetime of 3 ns, as a change in the rotational correlation time of 1 ns involves a difference of only 50 ps in the decay time of the numerator record. What can be said is that the chromophore sits tightly in the entire molecule, as no short times are observed (also not in 60% glycerol). Very fast motion of any greater extent is also excluded by the r_0 value close to 0.4. In the case of RSGFP, we observed slightly shorter correlation times and an r_0 of only 0.35. This may indicate increased chromophore flexibility and is likely related to the specific amino acid substitutions in RSGFP (in particular, the Ser 65 → Gly change, replacing Ser 65 with a much smaller group). Because of the photochromicity we could not measure anisotropy with excitation at 400 nm.

Some of the questions which led to this study have been answered; we believe we can distinguish the three states A, I, and B in time-resolved experiments, and we can understand the photochromicity as nonequilibration of species in the ground state after transformation in the excited state. On the other hand new questions have arisen, such as the assignment of the 850 ps component and its dependence upon the photohistory of the protein, so that further work can be pursued.

Acknowledgment. We thank Dr. R. Rivera-Pomar (MPIbpc, Göttingen, Germany) and Dr. D. Piston (Vanderbilt University, Nashville, TN) for gifts of mutant GFP plasmids. We thank Dr. Thomas M. Jovin for a critical reading of the manuscript. V.S. was a recipient of a postdoctoral fellowship from the Human Frontiers Science Program Organization (HFSPO).

References and Notes

(1) Ward, W. W.; Cody, C. W.; Hart, R. C.; Cormier, M. J. *Photochem. Photobiol.* **1980**, *31*, 611−615.
(2) Nageswara Rao, B. D.; Kemple, M. D.; Prendergast, F. G. *Biophys. J.* **1980**, *32*, 630−632.
(3) Chattoraj, M.; King, B. A.; Bublitz, G. U.; Boxer, S. G. *Proc. Natl. Acad. Sci. U.S.A.* **1996**, *93*, 8362−8367.
(4) Lossau, H.; Kummer, R. A.; Heinecke, F.; Pöllinger-Dammer, C.; Kompa, G.; Bieser, J. T.; Silva, C. M.; Yang, M. M.; Youvan, D. C.; Michel-Beyerle, M. E. *Chem. Phys.* **1996**, *213*, 1−16.
(5) Creemers, T.; Lock, A.; Subramaniam, V.; Jovin, T. M.; Völker, S. *Nature Struct. Biol.* **1999**, *6*, 557−560.
(6) Swaminathan, R.; Hoang, C. P.; Verkman, A. S. *Biophys. J.* **1997**, *72*, 1900−1907.
(7) Cubitt, A. B.; Heim, R.; Adams, S. R.; Boyd, A. E.; Gross, L. A.; Tsien, R. Y. *Trends Biochem. Sci.* **1995**, *20*, 448−455.
(8) Patterson, G. H.; Knobel, S. M.; Sharif, W. D.; Kain, S. R.; Piston, D. W. *Biophys. J.* **1997**, *73*, 2782−2790.
(9) Dickson, R. M.; Cubitt, A.; Tsien, R. Y.; Moerner, W. E. *Nature* **1997**, *388*, 355−358.
(10) Miyawaki, A.; Griesbeck, O.; Heim, R.; Tsien, R. Y. *Proc. Natl. Acad. Sci. U.S.A.* **1999**, *96*, 2135−2140.
(11) Delagrave, S.; Hawtin, R. E. Silva, C. M.; Yang, M. M.; Youvan, D. C. *Biotechnology* **1995**, *13*, 151−154.
(12) Striker, G. In *Deconvolution and Reconvolution of Analytic Signals*; Bouchy, M., Ed.; ENSIC-INPL: Nancy, 1982; pp 329−364.
(13) Striker, G.; Labuda, D; Vega-Martin, M. C. *J. Biomol. Struct. Dyn.* **1989**, *7*, 235−255.
(14) *Handbook of Tables for Probability and Statistics*, 2nd ed.; Beyer, W., Ed.; The Chemical Rubber Co.: Cleveland, 1968; p 414.
(15) Xu, C.; Zipfel, W.; Shear, J. B.; Williams, R. M.; Webb, W. W. *Proc. Natl. Acad. Sci. U.S.A.* **1996**, *93*, 10763−10768.
(16) Volkmer, A.; Subramaniam, V.; Birch, D. J. S.; Jovin, T. M. *Biophys. J.*, in press.
(17) Brejc, K.; Sixma, T. K.; Kitts, P. A.; Kain, S. R.; Tsien, R. Y.; Ormo, M.; Remington, S. J. *Proc. Natl. Acad. Sci. U.S.A.* **1997**, *94*, 2306−2311.
(18) Valeur, B.; Weber, G. *J. Chem. Phys.* **1978**, *69*, 2393−2400.
(19) Demchenko, A. P. In *Topics in Fluorescence Spectroscopy*; Lakowicz, J. R., Ed.; Plenum Press: New York, 1992; Vol. 3, Chapter 2.
(20) Bublitz, G.; King, B. A.; Boxer, S. G. *J. Am. Chem. Soc.* **1998**, *120* 9370−9371.
(21) Yang, F.; Moss, L. G.; Phillips, N. G. *Nature Biotech.* **1996**, *14*, 1246−1251.
(22) Ormo, M.; Cubitt, A. B.; Kallio, K.; Gross, L. A.; Tsien, R. Y.; Remington, S. J. *Science* **1996**, *273*, 1392−1395.